Advances in Concrete Construction, *Vol. 9, No. 6 (2020) 557-568*
DOI: https://doi.org/10.12989/acc.2020.9.6.557

Analytical vibration of FG cylindrical shell with ring support based on various configurations

Muzamal Hussain*[1] and Abdellatif Selmi[2,3]

[1]*Department of Mathematics, Govt. College University Faisalabad, 38000, Faisalabad, Pakistan*
[2]*Department of Civil Engineering, College of Engineering in Al-Kharj, Prince Sattam bin Abdulaziz University, Al-Kharj 11942, Saudi Arabia*
[3]*Ecole Nationale d'Ingénieurs de Tunis (ENIT), Civil Engineering Laboratory. B.P. 37, Le belvédère 1002, Tunis, Tunisia*

(*Received February 1, 2020, Revised May 25, 2020, Accepted March 26, 2020*)

Abstract. In this study, the impact of ring supports around the shell circumferential has been examined for their various positions along the shell axial length using Rayleigh-Ritz formulation. These shells are stiffened by rings in the tangential direction. For isotropic materials, the physical properties are same everywhere where the laminated and functionally graded materials, they vary from point to point. Here the shell material has been taken as functionally graded material. The influence of the ring supports is investigated at various positions. These variations have been plotted against the locations of ring supports for three values of length-to-diameter ratios. Effect of ring supports with middle layer thickness is presented using the Rayleigh-Ritz procedure with three different conditions. The influence of the positions of ring supports for clamped-clamped is more visible than simply supported and clamped-free end conditions. The frequency first increases and gain maximum value in the midway of the shell length and then lowers down. The Lagrangian functional is created by adding the energy expressions for the shell and rings. The axial modal deformations are approximated by making use of the beam functions. The comparisons of frequencies have been made for efficiency and robustness for the present numerical procedure. Throughout the computation, it is observed that the frequency behavior for the boundary conditions follow as; clamped-clamped, simply supported-simply supported frequency curves are higher than that of clamped-simply curves. To generate the fundamental natural frequencies and for better accuracy and effectiveness, the computer software MATLAB is used.

Keywords: Rayleigh-Ritz; MATLAB; Lagrangian functional; middle layer

1. Introduction

Study of vibration characteristics of cylindrical shells with ring supports is a widely area of research in applied mathematics and theoretical mechanics. Analytical investigation of vibrations of these shell are performed to estimate the probable dynamical response. Vibration shell problems with ring supports occur in industrial engineering fields. Their vibration analysis predicts to approximate the experimental results. Nature of a shell material plays an important role in specifying their vibration frequencies. Stability of a cylindrical shell depends highly on these aspects of material. More the shell material sustains a load due to physical situations, the more the shell is stable. Any predicted fatigue due to burden of vibrations is evaded by estimating their dynamical aspects.

Variations in the shell physical parameters are inducted to enhance their strength and stability. During the recent years, study of cylindrical shell (CSs) has gained the attention of researchers doing work on their vibration characteristics. Advanced composite materials keep extreme particular stiffness, strength and are resistant to corrosion. Firstly, Love (1888) presented the Kirchhoff's hypotheses for plates. After that this theory became a foundation stage for building new ones by changing physical terms expressions.

More than one form of materials is used to structure the functionally graded (FG) materials and their physical properties vary from one surface to the other surface. In these surfaces, one has highly heat resistance property while other may preserve great dynamical perseverance and differs mechanically and physically in regular manner from one surface to other surface, making them of dual physical appearance. All these materials have changeable outer and inner sides and their physical properties greatly differ from each other (Suresh and Mortensen 1997, Koizumi 1997). These materials are organized by various techniques and their applications are seen in dynamical elements such as plates, beams and shells. Moreover, they are also observed in space crafts, nuclear reactors and missiles technology etc. Sewall and Naumann (1968) considered the vibration analysis of CSs based on analytical and experimental methods. The shells were strengthened with longitudinal stiffeners. Xiang *et al.* (2002) formed some closed form solution functions for studying vibrations of cylindrical shells. The mid-way ring supports were clamped around the shells. Sharma (1974) analyzed vibration frequencies circular cylinder with using the Rayleigh - Ritz method (RRM) and made comparisons of his results with some experimental ones.

*Corresponding author, Research Scholar
E-mail: muzamal45@gmail.com,
muzamalhussain@gcuf.edu.pk

ISSN: 2287-5301 (Print), 2287-531X (Online)

Sharma *et al*. (1998) determined frequencies of composite cylindrical shells containing fluid. They estimated the axial modal deformations by trigonometric functions. Wang *et al*. (1997) scrutinized the vibrations of ring-stiffened CSs using Ritz polynomial functions. Materials of both shells and rings were of isotropic nature. These shells were stiffened with isotropic rings having three forms of locations on the shell outer surface. To increase the stiffness of CSs was stabilized by ring-stiffeners. Isotopic materials are the constituents of these rings. A large use of shell structures in practical applications makes their theoretical analysis an important field of structural dynamics. Since a shell problem is a physical one, so their vibrational behaviors are distorted by variations of physical and material parameters. Jiang and Olson (1994) recommended the characteristics of analysis of stiffened shell using finite element method to diminish large computational efforts which are required in the conventional finite element analysis. To elude any complications which may risk a physical system their analytical investigation was done. Ergin and Temarel (2002) did a vibration study of cylindrical shells. The shells lied in a horizontal direction and contained fluid and submerged in it. Najafizadeh and Isvandzibaei (2007) applied ring supports to CSs for vibration analysis along the tangential direction and founded their research on angular deformation theory of higher order. The angular deformation was used for shell equations and determined the effects of constituent volume fractions and shell configurations on the shell vibrations. FG material parameters were changed step by step.

Wang and Lai (2000) examined a novel approach for the evaluation of eigen - frequencies of cylindrical shells. The numerical process adopted by them was alike the wave propagation approach (WPA). Zhang (2002) studied vibrations of CSs submerged in a fluid. It was seen that the fluid factor impressed vibration shell frequencies to a significant limit. Shah *et al*. (2009) and Sofiyev and Avcar (2010) studied stability of CSs based on Rayleigh - Ritz and Galerkin technique using elastic foundations. The structures of cylindrical shell were tackled under the exponential law and axial load. Hussain and Naeem (2017) examined the frequencies of armchair tubes using Flügge's shell model. The effect of length and thickness-to-radius ratios against fundamental natural frequency with different indices of armchair tube was investigated. Hussain *et al*. (2017) demonstrated an overview of Donnell theory for the frequency characteristics of two forms of SWCNTs. Fundamental frequencies with different parameters have been investigated with WPA. Hussain and Naeem (2018) used Donnell's shell model to calculate the dimensionless frequencies for two forms of single-walled carbon nanotubes. The frequency influence was observed with different parameters. Pankaj *et al*. (2019) studied the functionally graded material using sigmoid law distribution under hygrothermal effect. The Eigen frequencies are investigated in detail. Frequency spectra for aspect ratios have been depicted according to various edge conditions. Several researchers used different approaches for the investigation of frequency of cylinders and concrete material (Kagimoto *et al*. 2015, Mesbah and Benzaid 2017, Alijani and Bidgoli 2018, Demir and Livaoglu 2019, Samadvand and Dehestani 2020).

According to our knowledge, up to now little is known about the vibration analyses of varying three layers in different configuration and has not been investigated for three layered FG-CS with ring supports based on Rayleigh-Ritz method. The proposed model is quite straightforward for the vibrational analysis of these structures of CSs. A large use of shell structures in practical applications makes their theoretical analysis an important field of structural dynamics. Since a shell problem is a physical one, so their vibrational behaviors are distorted by variations of physical and material parameters. It is also exhibited that the effect of frequencies by varying the different layers with constituent material. The frequencies changes with these layers according to the material formation of FG-CSs with ring supports. Throughout the computation, it is observed that the frequency behavior for the boundary conditions follow as; clamped-clamped (C-C), simply supported-simply supported (SS-SS) frequency curves are higher than that of clamped-simply (C-S) curves. Also the Sander's shell model based on the Rayleigh - Ritz method for estimating fundamental natural frequency has been developed to converge more quickly than other methods and models. The presented vibration modeling and analysis of CSs may be helpful especially in applications such as oscillators and in non-destructive testing. To elude any complications which may risk a physical system their analytical investigation is done.

2. Functionally graded material

The modeling of FG-CS is due to mixing two or more than two materials like ceramic and metal and the distribution of various functions and properties (physical and material), is termed as rule of mixture. Power law function has been utilized for with particular index using material properties in the thickness direction. The temperature and properties variations have been obtained by using the property of temperature and volume fraction. The distributions of volume fraction for all forms of CSs are assumed as (Chi and Chung 2006).

$$V_f = \left[\frac{z}{h} + \frac{1}{2}\right]^p \tag{1}$$

where p, h and z, respectively, denoted for power law index, thickness and the coordinate, where z which varies from zero to infinity.

A FG-CS consisting of two constituent materials. In these forms, nickel, stainless steel and zirconia are used for middle, internal and external surfaces, but their arrangement has profound influence on the formation of FG-CSs. If E_1 and E_2 as Young's moduli, v_1 and v_2 as Poisson's ratios, ρ_1 and ρ_2 mass densities respectively. Then effective material quantities for FG material are

$$E_{FGM} = \left[E_1 - E_2\right]\left[\frac{2z+h}{2h}\right]^p + E_2,$$

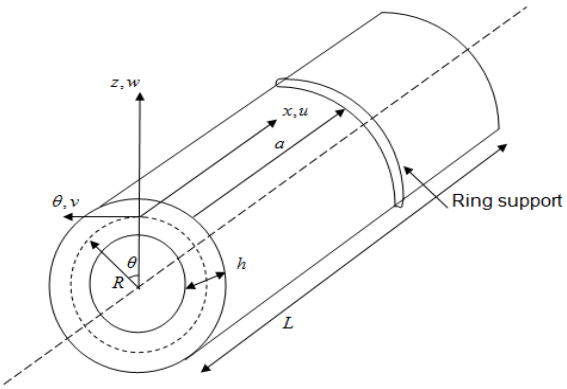

Fig. 1 Geometry of cylindrical shell with ring support

$$v_{FGM} = [v_1 - v_2]\left[\frac{2z+h}{2h}\right]^p + v_2,$$
$$\rho_{FGM} = [\rho_1 - \rho_2]\left[\frac{2z+h}{2h}\right]^p + \rho_2 \quad (2)$$

Toulokian *et al.* (1967) stated the material properties C at high temperature environ, with temperature-dependents which is a function of temperature. In Eq. (3), the constants (C_0,C_{-1},C_1,C_2,C_3) are different for different material.

$$C = C_0\left(C_{-1}T^{-1} + C_1T + C_2T^2 + C_3T^3\right) \quad (3)$$

3. Theoretical formation

The geometrical parameters L, h, R denotes as length, thickness and radius for CSs with its coordinate system (x, θ, z) as shown in Fig. 1. The x, θ co-ordinate are assumed to be along longitudinal and circumferential direction, respectively and z-co-ordinates are taken in its radial directions.

When the material and geometrical parameters are considered, the formula for a strain energy, S of a vibrating cylindrical shell is expressed as

$$S = \frac{R}{2}\int_0^L\int_0^{2\pi}[A_{11}e_1^2 + A_{22}e_2^2 + 2A_{12}e_1e_2 + A_{66}e_{12}^2 + 2(B_{11}e_1k_1 + B_{11}e_1k_1 + B_{11}e_1k_1 + B_{11}e_1k_1 + 2B_{66}e_{12}k_{12}) + D_{11}k_1^2 + D_{22}k_2^2 + 2D_{12}k_1k_2 + D_{66}^2k_{12}^2]d\theta dx \quad (4)$$

where e_1, e_2, e_3 and k_1 , k_2, k_3 designate the surface strains and curvatures respectively. The extensional stiffness, A_{ij} , coupling stiffness, B_{ij} and bending stiffness, D_{ij} are written as

$$\{A_{ij}, B_{ij}, D_{ij}\} = \int_{-h/2}^{h/2} Q_{ij}\{1, z, z^2\}dz (i, j = 1,2,6) \quad (5)$$

The variation of stiffness moduli A_{ij}, B_{ij}, D_{ij} $i.j = 1,2,6$ is modifies as

$$A_{ij} = A_{ij}^{in(Iso)} + A_{ij}^{m(FGM)} + A_{ij}^{ou(Iso)}$$
$$B_{ij} = B_{ij}^{in(Iso)} + B_{ij}^{m(FGM)} + B_{ij}^{ou(Iso)}$$
$$D_{ij} = D_{ij}^{in(Iso)} + D_{ij}^{m(FGM)} + D_{ij}^{ou(Iso)} \quad (6)$$

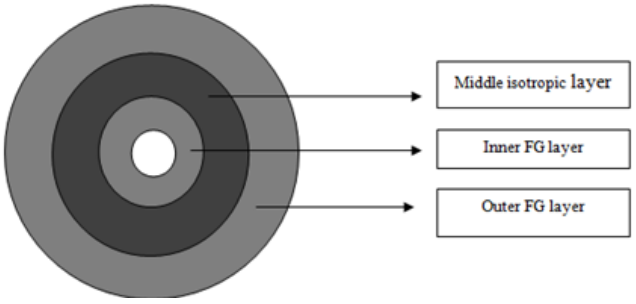

Fig. 2 Composition of material of CSs

Fig. 2 shows for the composition of layers with isotropic middle layers and other with FG layers.

Here the reduced stiffness, Q_{ij}'s are written as for isotropic CSs

$$Q_{11} = Q_{22} = \frac{E}{1-v^2}, \quad Q_{12} = \frac{vE}{1-v^2}, \quad Q_{66} = \frac{E}{2(1+v)} \quad (7)$$

The strain-displacement relations from Budiansky and Sanders (1963) furnished as

$$e_{12} = \frac{\partial y}{\partial x}, \quad e_{22} = \frac{1}{R}\left(\frac{\partial v}{\partial \theta} - w\right), \quad e_{12} = \frac{\partial v}{\partial x} + \frac{1}{R}\frac{\partial u}{\partial \theta} \quad (8)$$

and the expressions for the curvature - displacement relations are represented as

$$k_{11} = \frac{\partial^2 w}{\partial x^2}, \quad k_{22} = \frac{1}{R^2}\left(\frac{\partial^2 w}{\partial \theta^2} + \frac{\partial v}{\partial \theta}\right),$$
$$k_{12} = \frac{1}{R}\left(\frac{\partial^2 w}{\partial x \partial \theta} + \frac{3}{4}\frac{\partial v}{\partial x} - \frac{1}{4R}\frac{\partial u}{\partial \theta}\right) \quad (9)$$

Making substitutions of these relations from the expression (8) and (9) into the formula (4), the strain energy, S is takes the new forms

$$S = \frac{1}{2}\int_0^{2\pi L}\int_0^{} [A_{11}\left(\frac{\partial u}{\partial x}\right)^2 + A_{22}\frac{1}{R^2}\left(\frac{\partial v}{\partial \theta} + w\right)^2 + 2A_{12}\frac{1}{R}\frac{\partial u}{\partial x}\left(\frac{\partial v}{\partial \theta} + w\right) + A_{66}\left(\frac{\partial v}{\partial \theta} + \frac{1}{R}\frac{\partial u}{\partial x}\right)^2 - 2B_{11}\left(\frac{\partial u}{\partial x}\right)\left(\frac{\partial^2 w}{\partial x^2}\right) - 2B_{12}\frac{1}{R^2}\left(\frac{\partial u}{\partial x}\right)\left(\frac{\partial^2 w}{\partial \theta^2} - \frac{\partial v}{\partial \theta}\right) - 2B_{12}\frac{1}{R}\left(\frac{\partial v}{\partial \theta} + w\right)\left(\frac{\partial^2 w}{\partial x^2}\right) - 2B_{22}\frac{1}{R^3}\left(\frac{\partial v}{\partial \theta} + w\right)\left(\frac{\partial^2 w}{\partial \theta^2} - \frac{\partial v}{\partial \theta}\right) - 4B_{66}\frac{1}{R}\left(\frac{\partial v}{\partial \theta} + \frac{1}{R}\frac{\partial u}{\partial x}\right)\left(\frac{\partial^2 w}{\partial x \partial \theta} - \frac{3}{4}\frac{\partial v}{\partial x} + \frac{1}{4R}\frac{\partial u}{\partial \theta}\right) + D_{11}\left(\frac{\partial^2 w}{\partial x^2}\right)^2 + \frac{D_{22}}{R^4}\left(\frac{\partial^2 w}{\partial \theta^2} - \frac{\partial v}{\partial \theta}\right)^2 + 2D_{12}\frac{1}{R^2}\left(\frac{\partial^2 w}{\partial x^2}\right)\left(\frac{\partial^2 w}{\partial \theta^2} - \frac{\partial v}{\partial \theta}\right) + 4D_{66}\frac{1}{R^2}\left(\frac{\partial^2 w}{\partial x \partial \theta} - \frac{3}{4}\frac{\partial v}{\partial x} + \frac{1}{4R}\frac{\partial u}{\partial \theta}\right)^2]Rdxd\theta \quad (10)$$

The shell kinetic energy, K of the cylindrical shell is written as

$$K = \frac{1}{2}\iint_0^{2\pi L}\rho_t\left[\left(\frac{\partial u}{\partial t}\right)^2 + \left(\frac{\partial v}{\partial t}\right)^2 + \left(\frac{\partial w}{\partial t}\right)^2\right]Rdxd\theta \quad (11)$$

Where ρ_t is designated as

$$\rho_t = \int_{-h/2}^{h/2} \rho dz \tag{12}$$

The mass density ρ remains constant for an isotropic material. The Langrange energy functional $\prod$ for a vibrating cylindrical shell is stated as the difference between kinetic and strain energies and is expressed as

$$\prod = K - S \tag{13}$$

4. Solution methodology

Here Rayleigh's method is engaged to solve the CSs problem of differential equations in an efficient and comprehensive way. This method needs the axial modal approximates dependence on the characteristic function. The governing equation was formulated based on Sander's thin shell theory with energy functional. Over the past several years vibration of shell structures of various configurations and boundary conditions have been extensively studied (Hussain and Naeem 2019, Wang *et al.* 1997). The RRM is very powerful technique for the prediction of vibration of shells. Axial, circumferential and radial direction is related only to the axial displacement function. The unknown functions involving the tube dynamical equations are functions of shape linear variables. The independent variables are separated by employing prescribed method. They are supposed in the form of the product of separate functions of independent variables.

$$\begin{aligned} u(x,\theta,t) &= A_m \frac{d\phi}{dx}\cos n\theta \sin \omega t \\ v(x,\theta,t) &= B_m \phi(x) \sin n\theta \sin \omega t \\ w(x,\theta,t) &= C_m \phi(x) \prod_{i=1}^{N} (x-a_i)^{\varepsilon_i} \cos n\theta \sin \omega t \end{aligned} \tag{14}$$

Where A_m, B_m, C_m are taken as the displacement amplitudes in x, θ and z directions. The angular frequency and circumferential wave number are represented by ω and n respectivelywhere. The axial function $\phi(x)$ represents axial modal displacement shapes and satisfies the geometric boundary conditions. The term $x=a_i$ is the i^{th} ring supports along longitudinal direction and N, ε_i designates for number and existence of ring supports. When there is no ring on the shell the condition is $\varepsilon_i=0$ and for ring supports is $\varepsilon_i=1$.

The modified form of strain and kinetic energy with axial displacement functions

$$\begin{aligned} U = \frac{\pi R}{2}\int_0^L [& A_{11}A_m^2 \frac{d^2\varphi}{dx^2} + \frac{A_{22}}{R^2}\{nB_m\varphi + C_m\varphi(x-a)\}^2 \\ & + \frac{2A_{12}}{R}(A_m \frac{d^2\varphi}{dx^2})\{nB_m\varphi + C_m\varphi(x-a)\} \\ & + A_{66}(B_m \frac{d\varphi}{dx} - \frac{nA_m}{R}\frac{d\varphi}{dx})^2 - 2B_{11}(A_m \frac{d^2\varphi}{dx^2}) \\ & \{C_m(\frac{d^2\varphi}{dx^2}(x-a) + 2\frac{d\varphi}{dx})\} - \frac{2B_{12}}{R^2} \\ & (A_m \frac{d^2\varphi}{dx^2})\{-n^2 C_m\varphi(x-a) - nB_m\varphi\} \\ & - \frac{2B_{12}}{R}\{nB_m\varphi + C_m\varphi(x-a)\}\{C_m(\frac{d^2\varphi}{dx^2}(x-a) \\ & + 2\frac{d\varphi}{dx})\} - \frac{2B_{22}}{R^3}\{nB_m\varphi + C_m\varphi(x-a)\} \\ & \{-n^2 C_m\varphi(x-a) - nB_m\varphi\} - \frac{4B_{66}}{R}\{B_m \frac{d\varphi}{dx} \\ & - \frac{nA_m}{R}\frac{d\varphi}{dx}\}\{-nC_m(\frac{d\varphi}{dx}(x-a) + \varphi) - B_m \frac{d\varphi}{dx}\} \\ & + D_{11}\{C_m(\frac{d^2\varphi}{dx^2}(x-a) + 2\frac{d\varphi}{dx})\}^2 \\ & + \frac{D_{22}}{R^4}\{-n^2 C_m\varphi(x-a) - nB_m\varphi\}^2 + \frac{2D_{12}}{R^2} \\ & \{C_m(\frac{d^2\varphi}{dx^2}(x-a) + 2\frac{d\varphi}{dx})\}\{-n^2 C_m\varphi \\ & (x-a) - nB_m\varphi\} + \frac{4D_{66}}{R^2}\{-nC_m \\ & (\frac{d\varphi}{dx}(x-a) + \varphi) - B_m \frac{d\varphi}{dx}\}^2]\sin^2 \omega t dx \end{aligned} \tag{15}$$

and

$$T = \frac{\rho_t R\omega^2}{2}\int_0^L [A_m^2(\frac{d\varphi}{dx})^2 + B_m^2\varphi^2 + C_m^2\varphi^2(x-a)^2]\cos^2 \omega t dx \tag{16}$$

With the help of these equation, many (or any) ring supports can be investigated. For minimum energy principal, the relation of strain energy $U_{\max}$ and kinetic energy $T_{\max}$ are obtained, i.e.

$$\begin{aligned} U_{\max} = \frac{\pi R}{2}\int_0^L \Bigg[& A_{11}A_m^2\left(\frac{d^2\varphi}{dx^2}\right)^2 + \frac{n^2 A_{22}}{R^2}B_m^2\varphi^2 + \\ & \frac{A_{22}}{R^2}C_m^2(x-a)^2\varphi^2 + \frac{2nA_{22}}{R^2}B_m C_m(x-a) \\ & + \frac{2nA_{12}}{R}A_m B_m\varphi\frac{d^2\varphi}{dx^2} + \frac{2A_{12}}{R}A_m C_m(x-a)\varphi\frac{d^2\varphi}{dx^2} \\ & + A_{66}\left(B_m - \frac{n}{R}A_m\right)^2\left(\frac{d\varphi}{dx}\right)^2 \\ & - 2B_{11}A_m C_m(x-a)\left(\frac{d^2\varphi}{dx^2}\right)^2 - 4B_{11}A_m C_m\frac{d\varphi}{dx}\frac{d^2\varphi}{dx^2} \\ & + \frac{2n^2 B_{12}}{R^2}A_m C_m(x-a) \\ & \varphi\frac{d^2\varphi}{dx^2} + \frac{2nB_{12}}{R^2}A_m B_m\varphi\frac{d^2\varphi}{dx^2} - \frac{2nB_{12}}{R}B_m C_m(x-a)\varphi\frac{d^2\varphi}{dx^2} \\ & - \frac{4nB_{12}}{R}B_m C_m\varphi\frac{d\varphi}{dx} \\ & - \frac{2B_{12}}{R}C_m^2(x-a)^2\phi\frac{d^2\phi}{dx^2} - \frac{4B_{12}}{R}C_m^2(x-a)\phi\frac{d\phi}{dx} + \\ & \frac{2B_{22}}{R^3}(n^3 B_m C_m(x-a)\phi^2 \end{aligned}$$

$$+n^2B_m\varphi^2+n^2C_m^2(x-a)^2\varphi^2+nB_mC_m(x-a)^2\varphi)$$
$$+\frac{4B_{66}}{R}\left[nB_mC_m\left(\frac{d\varphi}{dx}\right)^2\right.$$
$$(x-a)+nB_mC_m\varphi\frac{d\varphi}{dx}+B_m^2\left(\frac{d\varphi}{dx}\right)^2-$$
$$\frac{n^2}{R}A_mC_m\left(\frac{d\varphi}{dx}\right)^2(x-a)-\frac{n^2}{R}A_mC_m\varphi\frac{d\varphi}{dx}$$
$$-\frac{n}{R}A_mB_m\left(\frac{d\varphi}{dx}\right)^2\Bigg]+D_{11}C_m^2\left[\left(\frac{d^2\varphi}{dx^2}\right)^2(x-a)^2+4\left(\frac{d\varphi}{dx}\right)^2+$$
$$4(x-a)\frac{d\varphi}{dx}\frac{d^2\varphi}{dx^2}\Bigg]+\frac{D_{22}}{R^4}\Bigg[n^4C_m^2(x-a)^2\varphi^2+n^2\varphi^2B_m^2$$
$$+2n^3B_mC_m(x-a)\varphi^2\Bigg]-\frac{2D_{12}}{R^2}\Bigg[n^2C_m^2\frac{d^2\varphi}{dx^2}$$
$$(x-a)^2\varphi+nB_mC_m(x-a)\varphi\frac{d^2\varphi}{dx^2}+$$
$$2n^2C_m^2(x-a)\varphi\frac{d\varphi}{dx}+2nB_mC_m\varphi\frac{d\varphi}{dx}\Bigg]$$
$$+\frac{4D_{66}}{R^2}\Bigg[n^2C_m^2(x-a)^2\left(\frac{d\varphi}{dx}\right)^2+n^2C_m^2\varphi^2+$$
$$2n^2C_m^2\varphi\frac{d\varphi}{dx}+B_m^2\left(\frac{d\varphi}{dx}\right)^2+2nB_mC_m$$
$$(x-a)\left(\frac{d\phi}{dx}\right)^2+2nB_mC_m\phi\frac{d\phi}{dx}\Bigg]\Bigg]\quad dx \tag{17}$$

and

$$T_{\max}=\frac{\pi R\rho_t\omega^2}{2}\int_0^L\left[A_m^2\left(\frac{d\varphi}{dx}\right)^2+B_m^2\varphi^2+C_m^2\varphi^2(x-a)^2\right]dx \tag{18}$$

Now, the Langrangian function can be written as

$$\Pi=T_{\max}-U_{\max}$$

The function is minimized with the help of vibration amplitudes A_m, B_m and C_m as:

$$\frac{\partial\Pi}{\partial A_m}=\frac{\partial\Pi}{\partial B_m}=\frac{\partial\Pi}{\partial C_m}=0$$

The compact form for three equations is

$$\left[A_{11}\int_0^L\left(\frac{d^2\varphi}{dx^2}\right)^2dx+\frac{n^2A_{66}}{R^2}\int_0^L\left(\frac{d\varphi}{dx}\right)^2dx\right]A_m+$$
$$\left[\frac{nA_{12}}{R}\int_0^L\varphi\frac{d^2\varphi}{dx^2}dx-\frac{nA_{66}}{R}\int_0^L\left(\frac{d\varphi}{dx}\right)^2dx+\frac{nB_{12}}{R^2}\right.$$
$$\left.\int_0^L\varphi\frac{d^2\varphi}{dx^2}dx-\frac{2nB_{66}}{R^2}\int_0^L\left(\frac{d\varphi}{dx}\right)^2dx\right]B_m+$$
$$\left[\frac{A_{12}}{R}\int_0^L(x-a)\varphi\frac{d^2\varphi}{dx^2}dx-B_{11}\int_0^L(x-a)\left(\frac{d^2\varphi}{dx^2}\right)^2dx\right.$$
$$-2B_{11}\int_0^L\left(\frac{d\varphi}{dx}\right)\left(\frac{d^2\varphi}{dx^2}\right)dx+\frac{n^2B_{12}}{R^2}$$
$$\int_0^L(x-a)\varphi\frac{d^2\varphi}{dx^2}dx-\frac{2n^2B_{66}}{R^2}\int_0^L\left(\frac{d\varphi}{dx}\right)^2dx-\frac{2n^2B_{66}}{R^2}$$
$$\left.\int_0^L\phi\frac{d\phi}{dx}dx\right]C_m=\rho_t\omega^2\int_0^L\left(\frac{d\phi}{dx}\right)^2dxA_m \tag{19}$$

$$\left[\frac{nA_{12}}{R}\int_0^L\varphi\frac{d^2\varphi}{dx^2}dx-\frac{nA_{66}}{R}\int_0^L\left(\frac{d\varphi}{dx}\right)^2dx+\frac{nB_{12}}{R^2}\int_0^L\varphi\frac{d^2\varphi}{dx^2}dx\right.$$
$$\left.-\frac{2nB_{66}}{R}\int_0^L\left(\frac{d\varphi}{dx}\right)^2dx\right]A_m+\left[\frac{n^2A_{22}}{R^2}\right.$$
$$\int_0^L\varphi^2dx+A_{66}\int_0^L\left(\frac{d\varphi}{dx}\right)^2dx+\frac{2n^2B_{22}}{R^3}\int_0^L\varphi^2dx+\frac{4B_{66}}{R}$$
$$\int_0^L\left(\frac{d\varphi}{dx}\right)^2dx+\frac{n^2D_{22}}{R^4}\int_0^L\varphi^2dx+\frac{4D_{66}}{R^2}$$
$$\left.\int_0^L\left(\frac{d\phi}{dx}\right)^2dx\right]B_m+\left[\frac{nA_{22}}{R^2}\int_0^L(x-a)\ \phi^2dx-\frac{nB_{12}}{R}\int_0^L(x-a)\right.$$
$$\phi\frac{d^2\phi}{dx^2}dx-\frac{2nB_{12}}{R}\int_0^L\phi\frac{d\phi}{dx}dx+\frac{n^3B_{22}}{R^3}$$
$$\int_0^L(x-a)\quad\phi^2dx+\frac{nB_{22}}{R^3}\int_0^L(x-a)\ \phi^2dx+$$
$$\frac{2nB_{66}}{R}\int_0^L(x-a)\left(\frac{d\phi}{dx}\right)^2+\frac{2nB_{66}}{R}\int_0^L\phi\frac{d\phi}{dx}dx+\frac{n^3D_{22}}{R^4}$$
$$\int_0^L(x-a)\ \phi^2dx-\frac{nD_{12}}{R^2}\int_0^L(x-a)\ \phi$$
$$\left.\frac{d^2\phi}{dx^2}dx-\frac{2nD_{12}}{R^2}\int_0^L\phi\frac{d\phi}{dx}dx+\frac{4nD_{66}}{R^2}\int_0^L(x-a)\left(\frac{d\phi}{dx}\right)^2dx\right.$$
$$\left.+\frac{4nD_{66}}{R^2}\int_0^L\phi\frac{d\phi}{dx}\right]C_m=\rho_t\omega^2\int_0^L\phi^2dxB_m \tag{20}$$

$$\left[\frac{A_{12}}{R}\int_0^L(x-a)\varphi\frac{d^2\varphi}{dx^2}dx-B_{11}\int_0^L(x-a)\left(\frac{d^2\varphi}{dx^2}\right)^2dx\right.$$
$$-2B_{11}\int_0^L\frac{d\varphi}{dx}\frac{d^2\varphi}{dx^2}dx+\frac{n^2B_{12}}{R^2}\int_0^L(x-a)\varphi$$
$$\left.\frac{d^2\varphi}{dx^2}dx-\frac{2n^2B_{66}}{R^2}\int_0^L(x-a)\left(\frac{d\varphi}{dx}\right)^2dx-\frac{2n^2B_{66}}{R^2}\int_0^L\varphi\frac{d\varphi}{dx}dx\right]A_m$$
$$+\left[\frac{nA_{22}}{R^2}\int_0^L(x-a)\varphi^2dx-\frac{nB_{12}}{R}\right.$$
$$\int_0^L(x-a)\varphi\frac{d^2\varphi}{dx^2}dx-\frac{2nB_{12}}{R}\int_0^L\varphi\frac{d\varphi}{dx}dx+\frac{n^3B_{22}}{R^3}\int_0^L(x-a)\varphi^2dx$$
$$+\frac{nB_{22}}{R^3}\int_0^L(x-a)\varphi^2dx+\frac{2nB_{66}}{R}$$
$$\left.\int_0^L(x-a)\left(\frac{d\varphi}{dx}\right)^2dx+\frac{2nB_{66}}{R}\int_0^L\varphi\frac{d\varphi}{dx}dx+\frac{n^3D_{22}}{R^4}\right.$$

Table 1 Convergence of RRM frequencies (Loy *et al*. 1997)

	Method	*n*			
		1	2	3	4
C-C	Loy *et al*. (1997)	0.032885	0.01393	0.02267	0.04221
	Present	0.034878	0.01405	0.02272	0.04227
S-S	Loy *et al*. (1997)	0.016101	0.00938	0.02211	0.04209
	Present	0.016102	0.00938	0.02211	0.04227
C-S	Loy *et al*. (1997)	0.023974	0.00822	0.00584	0.00871
	Present	0.024721	0.00828	0.00585	0.00871

$$\int_0^L (x-a)\varphi^2 dx - \frac{nD_{12}}{R^2}\int_0^L (x-a)\varphi\frac{d^2\varphi}{dx^2}dx - \frac{2nD_{12}}{R^2}\int_0^L \varphi\frac{d\varphi}{dx}dx + \frac{4nD_{66}}{R^2}\int_0^L (x-a)\left(\frac{d\varphi}{dx}\right)^2 dx + \frac{4nD_{66}}{R^2}\int_0^L \varphi\frac{d\varphi}{dx}dx\Bigg]B_m + \Bigg[\frac{A_{22}}{R^2}\int_0^L (x-a)^2\varphi^2 dx - \frac{2B_{12}}{R}\int_0^L (x-a)^2\varphi\frac{d^2\varphi}{dx^2}dx + \frac{4B_{12}}{R}\int_0^L (x-a)\varphi\frac{d\varphi}{dx} + \frac{2n^2B_{22}}{R^3}\int_0^L (x-a)^2\varphi^2 dx + D_{11}\int_0^L (x-a)^2\left(\frac{d^2\varphi}{dx^2}\right)^2 dx + 4D_{11}\int_0^L \left(\frac{d\varphi}{dx}\right)^2 dx + 4D_{11}\int_0^L (x-a)\frac{d\varphi}{dx}\frac{d^2\varphi}{dx^2}dx + \frac{n^4D_{22}}{R^4}\int_0^L (x-a)^2\varphi^2 dx - \frac{2n^2D_{12}}{R^2}\int_0^L (x-a)^2\varphi\frac{d^2\varphi}{dx^2}dx - \frac{4n^2D_{12}}{R^2}\int_0^L (x-a)\varphi\frac{d\varphi}{dx}dx + \frac{4n^2D_{66}}{R^2}\int_0^L (x-a)^2\left(\frac{d\varphi}{dx}\right)^2 dx + \frac{4n^2D_{66}}{R^2}\int_0^L \varphi^2 dx + \frac{8n^2D_{66}}{R^2}\int_0^L (x-a)\varphi\frac{d\varphi}{dx}dx\Bigg]C_m = \int_0^L \rho_t\omega^2\int_0^L (x-a)^2\varphi^2 dx C_m \tag{21}$$

The above equations can be written in the form of matrices as

$$\begin{bmatrix} a_{11} & a_{12} & a_{13} \\ a_{12} & a_{22} & a_{23} \\ a_{13} & a_{23} & a_{33} \end{bmatrix}\begin{bmatrix} A_m \\ B_m \\ C_m \end{bmatrix} = \rho_t\omega^2\begin{bmatrix} I_2 & 0 & 0 \\ 0 & I_9 & 0 \\ 0 & 0 & I_{11} \end{bmatrix} \tag{22}$$

The expressions for the terms $a_{ij}^{'}s$, I_2, I_9 and I_{11} are given in Appendix-I.

5. Simulation results and discussion

Here, the versatile numerical technique RRM has been used in current study to investigate the vibration of FG-CS with ring support. For the convergence rate of CSs, the non-dimensional frequency enumerated in the current work, i.e., using RRM are happened to be in a good consistency along with the so-called exact results furnished by Loy *et al*. (1997), those were established by working out with the deformation theory provided in Table 1. There is once again comparison of present resuts of CSs with Loy *et al*. (1999), Ansari *et al*.(2011) and Warburton (1965), provided in Fig. 3(a) and Gonclaves *et al*. (2006), Gonclaves and Batista (1988), Gaser (1987) as shown in Fig 3(b). The proposed model based on RRM can incorporate in order to accurately predict the acquired results of material data point. Fig. 4 indicates that the frequency values versus circumferential wave number. It is observed that the frequencies are highly visible for without ring are higher than those for ones. In Fig. 4, variations of frequencies are shown versus the wave modes (*n*). As *n* grows, frequencies for cylindrical shells boost indefinitely.

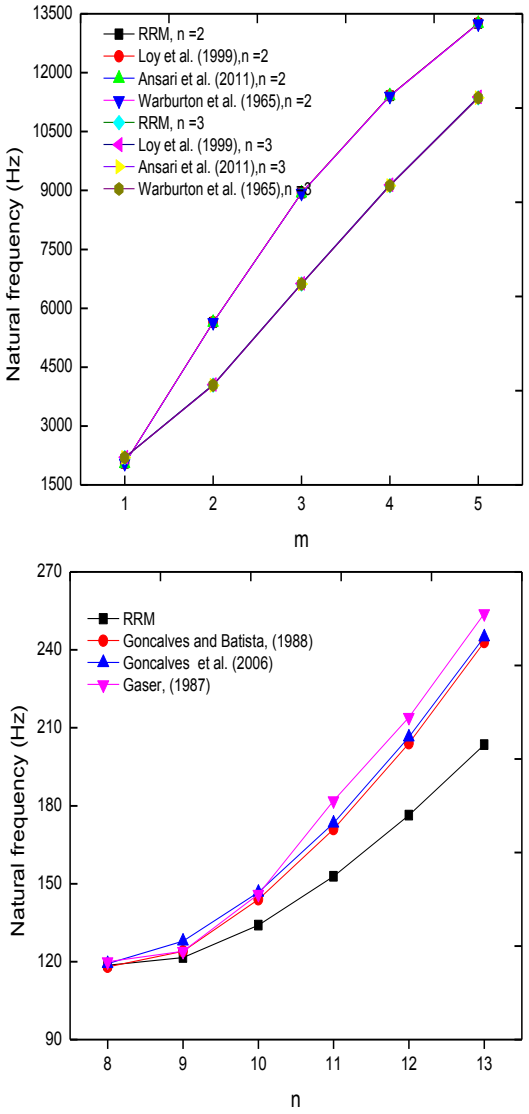

Fig. 3 Convergence of RRM frequencies (a) versus *m* (*n*=1, *L*=8 in, *h*=0.1 in, *R*=*2* in, *E*=30×10^6 lbf in^{-2}, *v*=0.3, *ρ*=7.35×10^{-4} lbf s^2 in^{-4}) (b) versus *n* (*m*=1, *L*=0.41 m, *h*=0.001 m, *R*=0.3015 m, *E*=2.1×10^{11} N/m^2, *v*=0.3, *ρ*=7850 Kg/m^3)

Table 2 Configuration of layers with materials as Stainless Steel (STS), Zirconia (ZI) and Nickel (NI)

Layers	Configurations			
	Form I	Form II	Form III	Form IV
Inner layer (Iso)	STS -ZI	STS - ZI	ZI -STS	ZI - STS
Middle layer (FGM)	NI	NI	NI	NI
Outer layer (Iso)	STS - ZI	ZI - STS	STS - ZI	ZI - STS

Table 3 Configuration of layers with thickness

Layers	Configurations			
	Form I	Form II	Form III	Form IV
Inner layer (Iso)	5*h*/12	*h*/4	*h*/4	*h*/6
Middle layer (FGM)	*h*/6	*h*/4	*h*/4	2*h*/3
Outer layer (Iso)	5*h*/12	*h*/2	*h*/2	*h*/6

Table 4 Comparison of C-C frequencies for all forms of shell versus circumferential wave numbers (*n*)

p	*n*	Form I	Form II	Form III	Form IV
3	1	662.27	647.28	648.26	635.13
	2	439.62	429.50	430.76	421.89
	3	336.21	328.01	330.26	323.04
	4	336.22	327.13	331.99	323.97
5	1	685.58	662.82	663.64	644.73
	2	455.03	439.84	440.95	428.31
	3	347.80	336.03	337.87	328.11
	4	347.44	335.36	339.27	329.36
7	1	702.42	671.03	671.75	649.62
	2	463.53	445.31	446.30	431.58
	3	354.19	340.30	341.84	330.70
	4	353.61	339.82	342.98	332.11

Table 5 Frequency comparison for all forms of shell versus circumferential wave numbers (*n*) with C-S.

p	*n*	Form I	Form II	Form III	Form IV
3	1	596.97	583.55	583.82	572.08
	2	347.74	339.80	340.08	333.11
	3	246.77	240.60	242.46	237.03
	4	276.45	268.63	273.64	266.74
5	1	617.99	597.57	597.67	580.71
	2	359.95	347.98	348.12	338.17
	3	255.22	246.54	247.98	240.80
	4	285.53	275.49	279.50	271.29
7	1	629.57	604.97	604.98	585.11
	2	366.68	352.30	352.36	340.75
	3	259.87	249.71	250.85	242.72
	4	290.52	279.22	282.45	273.61

Table 6 Comparison of SS-SS frequencies for all forms of shell versus circumferential wave numbers (*n*)

p	*n*	Form I	Form II	Form III	Form IV
3	1	350.96	343.10	343.70	336.20
	2	170.03	166.10	166.21	162.77
	3	147.79	143.75	146.09	142.53
	4	227.92	221.19	226.48	220.55
5	1	363.32	350.36	351.20	341.28
	2	175.98	170.11	170.12	165.25
	3	152.71	147.38	149.27	144.91
	4	235.30	226.91	231.21	224.40
7	1	370.13	355.72	355.84	343.87
	2	179.26	172.23	172.81	166.52
	3	155.41	149.35	150.89	146.13
	4	239.35	230.03	233.57	226.37

Since a FG-CS is composed of three layers having different thickness for different four forms, which is presented in the Tables 2 and 3.

5.1 Frequency behavior without ring supports for all forms of CSs

In Tables 4-6, frequencies of vibrating FG-CSs are plotted versus the wave number, *n*. These frequencies have been examined for the wave number, *m*=1. These tables portray the variations of frequencies with circumferential wave number, *n* for all forms of shell. These variations of the natural frequency (Hz) have been calculated for the following volume fraction exponents: *p*=3, 5, 7 of FGM cylindrical shells. The frequencies first decrease then increase for all forms of shell as *n* increases and frequencies increases on increases the law exponent. In these tables, for clamped-clamped conditions, variations of frequencies are higher than that of other conditions.

5.2 Frequency variation of isotropic middle layer with ring supports

In Fig. 5, frequencies of vibrating CSs with ring support are plotted versus the wave number, *n*. These variations of the natural frequency (Hz) have been calculated for the four forms with volume fraction exponent *p*=0.5. Figures depicts that frequencies increases with the increase of *n* with ring attached at *a/L*=0.1 The frequencies diminishes on increasing the middle layer thickness and the effect ring support is prominent with three different boundary conditions. For clamped-clamped conditions, variations of frequencies are higher than that of other conditions.

Here frequencies for four forms of FG-CSs with ring supports are presented in following figures. The frequency variation with the position of the ring support at *a/L*=0.3 for the edge conditions: SS- SS, C-C and C-S for both FG-CS as shown in Fig. 6-8. These figures depicts the frequency variations versus ring support for four forms of cylindrical shell with for three values of *L/R*=10, 15, 20 and law exponent is 0.5 (*m*=1, *n*=1, *h/R*=0.002). These variations of frequencies are drawn with three forms of end conditions. As *a* is enhanced for these boundary conditions, the frequencies go up. At *a/L* (=0.5) all the frequencies are higher and at *a/L* (=0.6~0.9), the frequencies decreases. The frequencies are same at *a/L*=0, 1 and rust itself a bell shape. In these figure, the C-S are lower than that of C-C and SS-SS. As shown by this figure, the boundary conditions C-C have the highest frequency curves. These frequencies have a great impact on the vibration of CSs. It is inferred this frequency behavior with position of the ring supports has paramount influence on the vibrations of FG-CSs. From

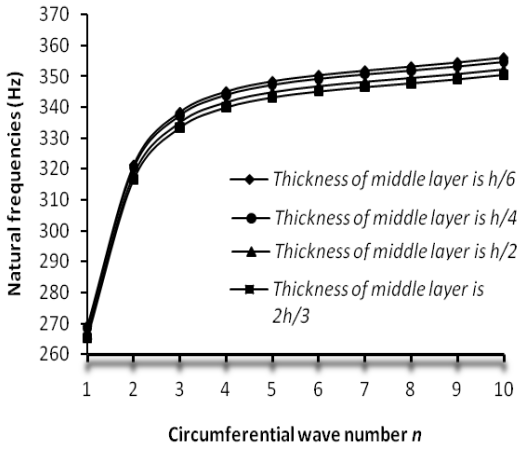

(C-C)

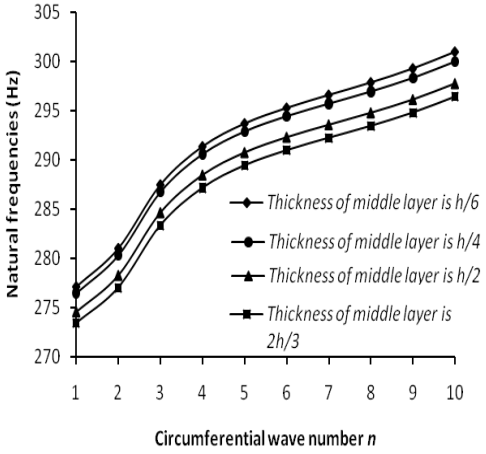

(C-S)

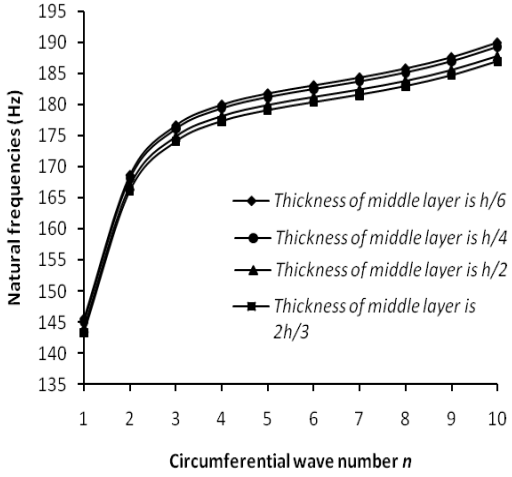

(SS-SS)

Fig. 5 Frequency variations for middle isotropic layer of C-C, C-S, SS-SS versus (*n*)

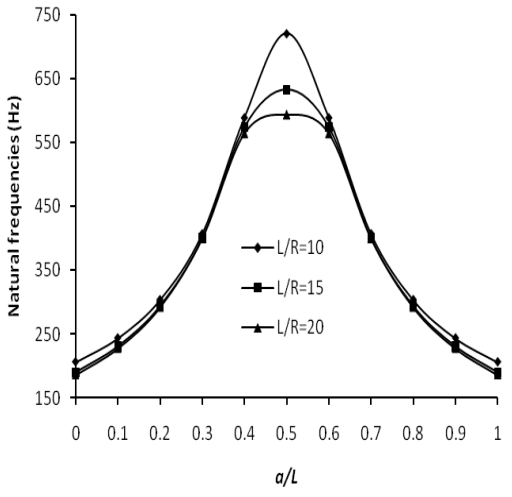

(Form-I)

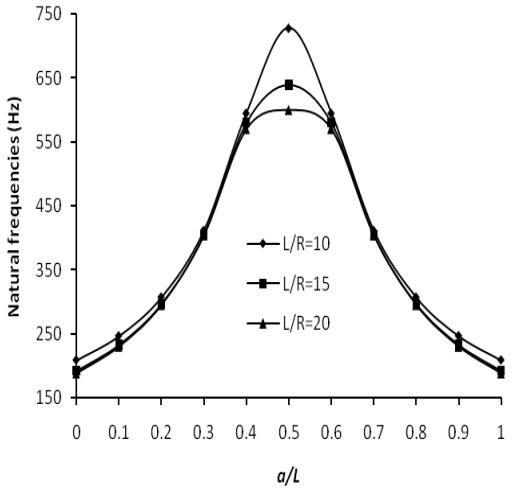

(Form-II)

Fig. 6 Variations of frequency with *L/R* ratios of SS-SS condition versus ring support (a) Form-I (b) Form-II (c) Form-III (d) Form-IV)

these figures, it can be seen that the frequency behavior versus position of ring position at *a/L* (=0~0.5) for form I and II with *L/R*=10 for C-C is 71.4%, SS-SS is 60.3% and with *L/R*=15 for C-C is 70%, SS-SS is 59.6% and with *L/R*=20 for C-C is 68.6%, SS-SS is 59.2%. Now frequency variation for form III and form Iv is calculated as with *L/R*=10 for C-C is 71.5%, SS-SS is 60.7%, and with *L/R*=15 for C-C is 70.2%, SS-SS is 60% and with *L/R*=20 for C-C is 68.9%, SS-SS is 59.5%. The interesting phenomena occurs for the C-S condition that the frequencies are symmetrical

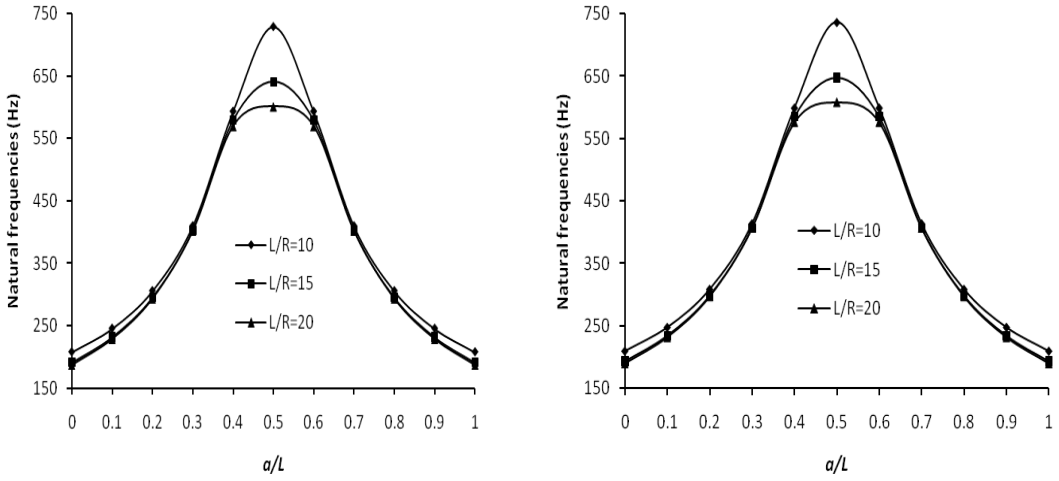

(Form-III) (Form-IV)

Fig. 6 Continued

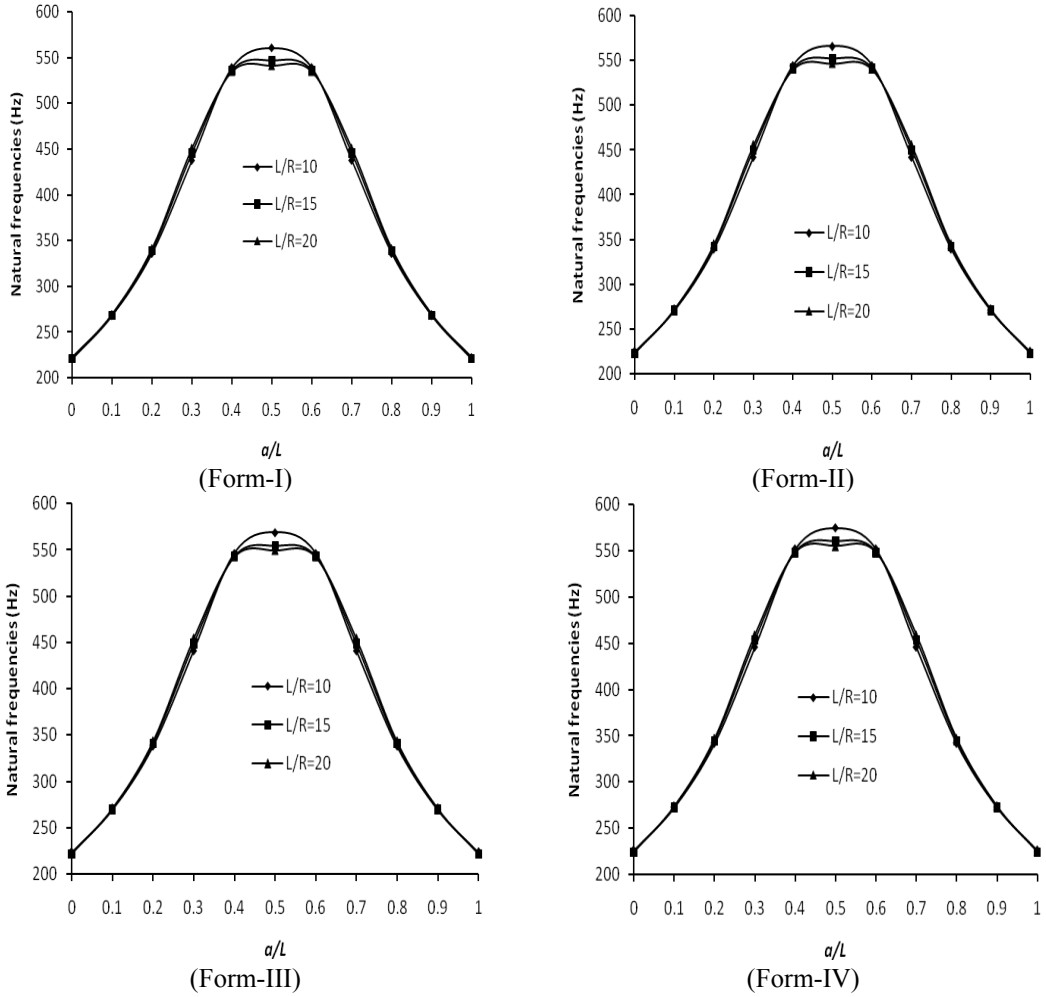

(Form-I) (Form-II)

(Form-III) (Form-IV)

Fig. 7 Variations of frequency with *L/R* ratios of SS-SS condition versus ring support (a) Form-I (b) Form-II (c) Form-III (d) Form-IV)

about the center for all forms of shell configuration, shown in Fig. 8.

6. Conclusions

In present study, vibrations of FG cylindrical shells have been examined for four forms of cylindrical shell. Theoretical study gives a prediction to estimate experimental frequencies and avoids any future risk to a physical system. For the derivation of frequency equation,

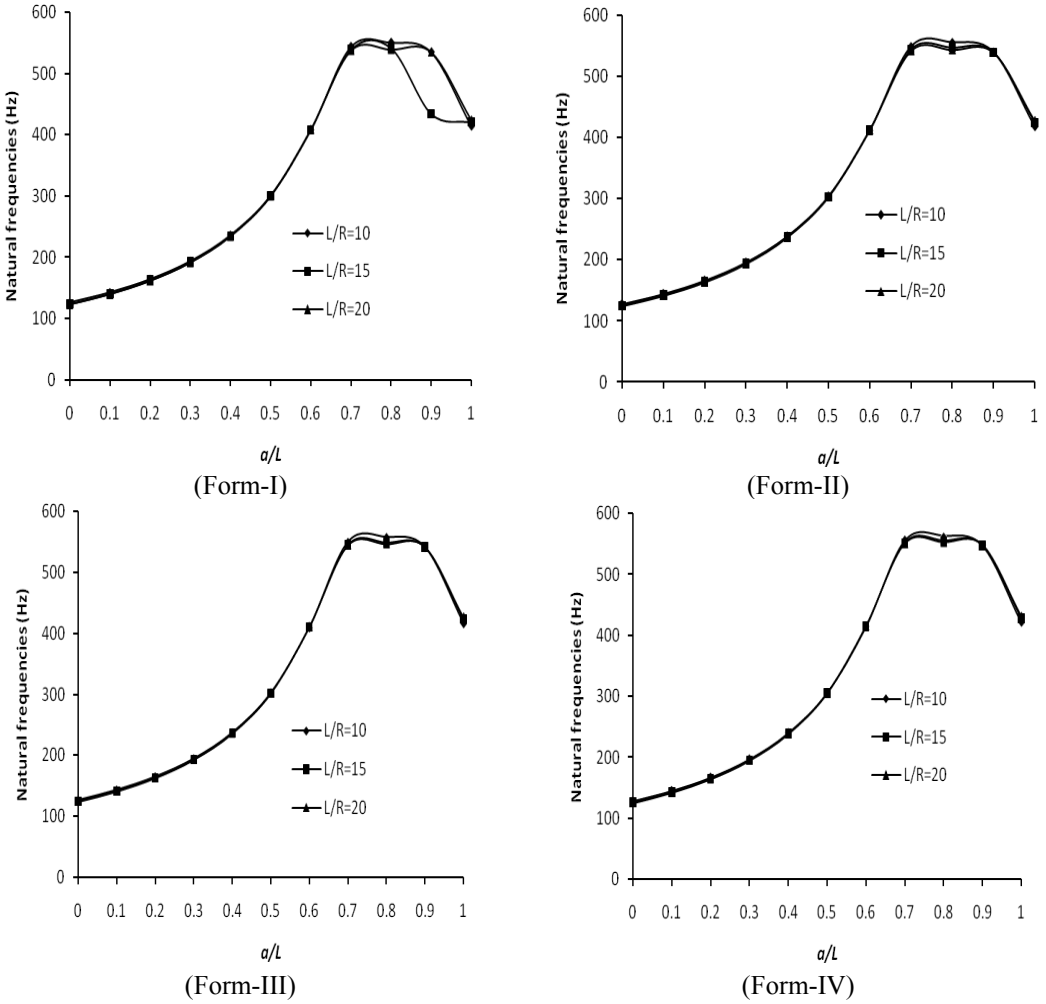

Fig. 8 Variations of frequency with *L/R* ratios of C-S condition versus ring support (a) Form-I (b) Form-II (c) Form-III (d) Form-IV)

Rayleigh-Ritz technique has been applied. Terms of ring supports have been introduced by a polynomial function that bears the degree equal to the number of ring supports. These results have been obtained for circumferential wave mode for different layers with various ratios of length-to-radius. Variations of frequencies with the locations of ring supports have been analyzed placed round the circumferential direction. The position of a ring support has been taken along the shell length. It is seen that frequencies increases on inducting of ring-position and play prominent role in the shell vibration. The frequency first increases and obtains its maximum value at the shell mid length position and then decreases and get a bell shape for clamped-clamped and simply supported conditions. In clamped-simply supported, frequencies are symmetrical about the center of the shell and not form the shape of bell. The frequency behaviors have been fully checked with different material and configuration of four forms of shells. The frequency decreases from first shell to forth shell due to the configuration and shell thickness variations. Also the effect of middle layer has been seen in very prominent manners. Its values at both ends are similar. This procedure can be applied to vibration characteristics of FG-shell using various volume fraction laws with ring supports.

Declaration of Conflicting Interests

The author(s) declared no potential conflicts of interest with respect to the research, authorship, and/or publication of this article.

References

Alijani, M. and Bidgoli, M.R. (2018), "Agglomerated SiO_2 nanoparticles reinforced-concrete foundations based on higher order shear deformation theory: Vibration analysis", *Adv. Concrete Constr.*, **6**(6), 585. https://doi.org/10.12989/acc.2018.6.6.585.

Arshad, S.H., Naeem, M.N. and Sultana, N. (2007). "Frequency analysis of functionally graded cylindrical shells with various volume fraction laws", *J. Mech. Eng. Sci.*, **221**, 1483-1495. https://doi.org/10.1243/09544062JMES738.

Asghar, S., Hussain, M. and Naeem, M. (2019), "Non-local effect on the vibration analysis of double walled carbon nanotubes based on Donnell shell theory", *Physica E: Low Dimens. Syst. Nanostr.*, **116**, 113726. https://doi.org/10.1016/j.physe.2019.113726.

Chi, S.H. and Chung, Y.L. (2006), "Mechanical behavior of functionally graded material plates under transverse load-part II: numerical results", *Int. J. Solid. Struct.*, **43**, 3657-3691. https://doi.org/10.1016/j.ijsolstr.2005.04.010.

Demir, A.D. and Livaoglu, R. (2019), "The role of slenderness on the seismic behavior of ground-supported cylindrical silos", *Adv. Concrete Constr.*, **7**(2), 65. https://doi.org/10.12989/acc.2019.7.2.065.

Dong S.B. (1977), "A block-stodola eigen solution technique for large algebraic systems with non-symmetrical matrices", *Int. J. Numer. Meth. Eng.*, **11**, 247. https://doi.org/10.1002/nme.1620110204.

Ergin, A. and Temarel, P. (2002), "Free vibration of a partially liquid-filled and submerged, horizontal cylindrical shell", *J. Sound Vib.*, **254**(5), 951-965. https://doi.org/10.1006/jsvi.2001.4139.

Goncalves, P.B. and Batista, R.C. (1988), "Non-linear vibration analysis of fluid-filled cylindrical shells", *J. Sound Vib.*, **127**(1), 133-143. https://doi.org/10.1016/0022-460X(88)90354-9.

Gonçalves, P.B., Silva, F. and del Prado, Z.J. (2006), "Transient stability of empty and fluid-filled cylindrical shells", *J. Braz. Soc. Mech. Sci. Eng.*, **28**(3), 331-333. https://doi.org/10.1590/S1678-58782006000300011.

Hussain, M. and Naeem, M. (2017), "Vibration analysis of single-walled carbon nanotubes using wave propagation approach", *Mech. Sci.*, **8**(1), 155-164. https://doi.org/10.5194/ms-8-155-2017.

Hussain, M., Naeem, M., Shahzad, A. and He, M. (2017), "Vibrational behavior of single-walled carbon nanotubes based on cylindrical shell model using wave propagation approach", *AIP Adv.*, **7**(4), 045114. https://doi.org/10.1063/1.4979112.

Hussain. M. and Naeem, M. (2018), "Vibration of single-walled carbon nanotubes based on Donnell shell theory using wave propagation approach", Chapter, Intechopen, Novel Nanomaterials - Synthesis and Applications, ISBN 978-953-51-5896-7.

Jiang, J. and Olson, M.D. (1994), "Vibrational analysis of orthogonally stiffened cylindrical shells using super elements", *J. Sound Vib.*, **173**, 73-83. https://doi.org/10.1006/jsvi.1994.1218.

Kagimoto, H., Yasuda, Y. and Kawamura, M. (2015), "Mechanisms of ASR surface cracking in a massive concrete cylinder", *Adv. Concrete Constr.*, **3**(1), 39. https://doi.org/10.12989/acc.2015.3.1.039.

Koizumi, M. (1997), "FGM Activities in Japan", *Compos. Part B: Eng.*, **28**(1-2), 1-4. https://doi.org/10.1016/S1359-8368(96)00016-9.

Lam, K.Y. and Loy, C.T. (1998), "Influence of boundary conditions for a thin laminated rotating cylindrical shell", *Compos. Struct.*, **41**, 215-228. https://doi.org/10.1016/S0263-8223(98)00012-9.

Loy, C.T. and Lam, K.Y. (1997), "Vibration of cylindrical shells with ring supports", *J. Mech. Eng.*, **39**, 455-471. https://doi.org/10.1016/S0020-7403(96)00035-5.

Loy, C.T., Lam, K.L. and Shu, C. (1997), "Analysis of cylindrical shells using generalized differential quadrature", *Shock Vib.*, **4**(3), 193-198. https://doi.org/10.3233/SAV-1997-4305.

Loy, C.T., Lam, K.Y. and Reddy, J.N. (1999), "Vibration of functionally graded cylindrical shells", *Int. J. Mech. Sci.*, **41**, 309-324. https://doi.org/10.1016/S0020-7403(98)00054-X.

Mesbah, H.A. and Benzaid, R. (2017), "Damage-based stress-strain model of RC cylinders wrapped with CFRP composites", *Adv. Concrete Constr.*, **5**(5), 539. https://doi.org/10.12989/acc.2017.5.5.539.

Naeem, M.N., Ghamkhar, M., Arshad, S.H. and Shah, A.G. (2013), "Vibration analysis of submerged thin FGM cylindrical shells", *J. Mech. Sci. Technol.*, **27**(3), 649-656. https://doi.org/10.1007/s12206-013-0119-6.

Najafizadeh, M.M. and Isvandzibaei, M.R. (2007), "Vibration of (FGM) cylindrical shells based on higher order shear deformation plate theory with ring support", *Acta Mechanica*, **191**, 75-91. https://doi.org/10.1007/s00707-006-0438-0.

Samadvand, H. and Dehestani, M. (2020), "A stress-function variational approach toward CFRP-concrete interfacial stresses in bonded joints", *Adv. Concrete Constr.*, **9**(1), 43-54. https://doi.org/10.12989/acc.2020.9.1.043.

Sewall, J. L. and Naumann, E. C. (1968), "An experimental and analytical vibration study of thin cylindrical shells with and without longitudinal stiffeners", National Aeronautic and Space Administration; for sale by the Clearinghouse for Federal Scientific and Technical Information, Springfield, VA..

Shah, A.G., Mahmood, T. and Naeem, M.N. (2009), "Vibrations of FGM thin cylindrical shells with exponential volume fraction law", *Appl. Math. Mech.*, **30**(5), 607-615. https://doi.org/10.1007/s10483-009-0507-x.

Sharma, C.B. and Johns, D.J. (1971), "Vibration characteristics of a clamped-free and clamped-ring-stiffened circular cylindrical shell", *J. Sound Vib.*, **14**(4), 459-474. https://doi.org/10.1016/0022-460X(71)90575-X.

Sharma, C.B., Darvizeh, M. and Darvizeh, A. (1998), "Natural frequency response of vertical cantilever composite shells containing fluid", *Eng. Struct.*, **20**(8), 732-737. https://doi.org/10.1016/S0141-0296(97)00102-8.

Sharma, P., Singh, R. and Hussain, M. (2019), "On modal analysis of axially functionally graded material beam under hygrothermal effect", *Proc. Inst. Mech. Eng., Part C: J. Mech. Eng. Sci.*, **234**(5), 1085-1101. https://doi.org/10.1177/0954406219888234.

Sodel W. (!981), *Vibration of Shell and Plates, Mechanical Engineering Series*, Marcel Dekker, New York.

Sofiyev, A.H. and Avcar, M. (2010), "The stability of cylindrical shells containing an FGM layer subjected to axial load on the Pasternak foundation", *Eng.*, **2**(4), 228. https://doi.org/10.4236/eng.2010.2403.

Suresh, S. and Mortensen, A. (1997), "Functionally gradient metals and metal ceramic composites, Part 2: Thermo mechanical behavior", *Int. Mater.*, **42**, 85-116.

Toulokian, Y.S. (1967), *Thermo Physical Properties of High Temperature Solid Materials*, Macmillan, New York.

Wang, C. and Lai, J.C.S. (2000), "Prediction of natural frequencies of finite length circular cylindrical shells", *Appl. Acoust.*, **59**(4), 385-400. https://doi.org/10.1016/S0003-682X(99)00039-0.

Wang, C.M., Swaddiwudhipong, S. and Tian, J. (1997), "Ritz method for vibration analysis of cylindrical shells with ring-stiffeners", *J. Eng. Mech.*, **123**, 134-143. https://doi.org/10.1061/(ASCE)0733-9399(1997)123:2(134).

Wuite, J. and Adali, S. (2005), "Deflection and stress behavior of nanocomposite reinforced beams using a multiscale analysis", *Compos. Struct.*, **71**(3-4), 388-396. https://doi.org/10.1016/j.compstruct.2005.09.011.

Xiang, Y., Ma, Y.F., Kitipornchai, S. and Lau, C.W.H. (2002), "Exact solutions for vibration of cylindrical shells with intermediate ring supports", *Int. J. Mech. Sci.*, **44**(9), 1907-1924. https://doi.org/10.1016/S0020-7403(02)00071-1.

Xuebin, L. (2008), "Study on free vibration analysis of circular cylindrical shells using wave propagation", *J. Sound Vib.*, **311**, 667-682. https://doi.org/10.1016/j.jsv.2007.09.023.

Zhang, X.M. (2002), "Parametric analysis of frequency of rotating laminated composite cylindrical shells with the wave propagation approach", *Comput. Meth. Appl. Mech. Eng.*, **191**, 2057-2071. https://doi.org/10.1016/S0045-7825(01)00368-1.

CC

Appendix-I

$$a_{11} = A_{11}I_1 + \left(\frac{n}{R}\right)^2 A_{66}I_2,$$

$$a_{12} = \left(\frac{n}{R}\right)\left(A_{12} + \frac{B_{12}}{R}\right)I_3 - \left(\frac{n}{R}\right)\left(A_{66} + \frac{2B_{66}}{R}\right)I_2,$$

$$a_{13} = \left(\frac{1}{R}\right)\left(A_{12} + \frac{n^2B_{12}}{R}\right)I_5 - B_{11}I_6 - 2\left(\frac{n}{R}\right)^2 B_{66}I_7,$$

$$a_{21} = \left(\frac{n}{R}\right)\left(A_{12} + \frac{B_{12}}{R}\right)I_3 - \left(\frac{n}{R}\right)\left(A_{66} + \frac{2B_{66}}{R}\right)I_2,$$

$$a_{22} = \left(\frac{n}{R}\right)^2\left(A_{22} + \frac{2B_{22}}{R} + \frac{D_{22}}{R^2}\right)I_4 + \left(A_{66} + \frac{4B_{66}}{R} + \frac{4D_{66}}{R^2}\right)I_2,$$

$$a_{23} = -\left(\frac{n}{R^2}\right)\left(A_{22} + \frac{(n^2+1)B_{22}}{R} + \frac{n^2D_{22}}{R^2}\right)I_8 + \left(\frac{n}{R}\right)\left(B_{12} + \frac{D_{12}}{R}\right)I_9 - \left(\frac{2n}{R}\right)\left(B_{66} + \frac{2D_{66}}{R}\right)I_7,$$

$$a_{31} = \left(\frac{1}{R}\right)\left(A_{12} + \frac{n^2B_{12}}{R}\right)I_5 - B_{11}I_6 - 2\left(\frac{n}{R}\right)^2 B_{66}I_7,$$

$$a_{32} = -\left(\frac{n}{R^2}\right)\left(A_{22} + \frac{(n^2+1)B_{22}}{R} + \frac{n^2D_{22}}{R^2}\right)I_8 + \left(\frac{n}{R}\right)\left(B_{12} + \frac{D_{12}}{R}\right)I_9 - \left(\frac{2n}{R}\right)\left(B_{66} + \frac{2D_{66}}{R}\right)I_7,$$

$$a_{33} = \left(\frac{1}{R^2}\right)\left(A_{22} + \frac{2n^2B_{22}}{R} + \frac{n^4D_{22}}{R^2}\right)I_{10} - \left(\frac{2}{R}\right)\left(B_{12} + \frac{n^2D_{12}}{R}\right)I_{11} + D_{11}I_{12} + 4\left(\frac{n}{R}\right)^2 D_{66}I_{13},$$

Where

$$I_1 = \int_0^L \left(\frac{d^2\varphi}{dx^2}\right)^2 dx$$

$$I_2 = \int_0^L \left(\frac{d\varphi}{dx}\right)^2 dx$$

$$I_3 = \int_0^L \varphi\frac{d^2\varphi}{dx^2}dx$$

$$I_4 = \int_0^L (x-a)\varphi\frac{d^2\varphi}{dx^2}dx$$

$$I_5 = \int_0^L (x-a)\left(\frac{d^2\varphi}{dx^2}\right)^2 dx$$

$$I_6 = \int_0^L \left(\frac{d\varphi}{dx}\right)\left(\frac{d^2\varphi}{dx^2}\right)dx$$

$$I_7 = \int_0^L (x-a)\left(\frac{d\phi}{dx}\right)^2 dx$$

$$I_8 = \int_0^L \phi\frac{d\phi}{dx}dx$$

$$I_9 = \int_0^L \phi^2 dx$$

$$I_{10} = \int_0^L (x-a)\phi^2 dx$$

$$I_{11} = \int_0^L (x-a)^2\phi^2 dx$$

$$I_{12} = \int_0^L (x-a)^2\phi\frac{d^2\phi}{dx^2}dx$$

$$I_{13} = \int_0^L (x-a)\phi\frac{d\phi}{dx}dx$$

$$I_{14} = \int_0^L (x-a)^2\left(\frac{d^2\phi}{dx^2}\right)^2 dx$$

$$I_{15} = \int_0^L (x-a)\frac{d\phi}{dx}\frac{d^2\phi}{dx^2}dx$$

$$I_{16} = \int_0^L (x-a)^2\left(\frac{d\phi}{dx}\right)^2 dx$$